



Fermilab

Fermi National Accelerator Laboratory
 Technical Support Engineering
 P.O. Box 500 - Batavia, Illinois - 60510



November 13, 1990

TO: SSC 50mm File

FROM: Jim Kerby, TS / Engineering

SUBJECT: Mechanical Analysis of the Vertically Split 50mm SSC Dipole

This paper presents results for finite element analyses of the vertically split yoke design for the 50mm SSC dipole, based on coil cross section W6733¹. The results were first presented at the May 23, 1990 SSC Dipole Task Force meeting, at Brookhaven National Laboratory. The results for the horizontally split design, the BNL baseline dipole design, have been reported elsewhere². Although related, and similar in appearance, the mechanics of the two designs are quite different. Rather than trying to ensure collar to yoke contact around the whole interface, the vertical split design only ensures contact at the horizontal region of the collar, leaving a clearance at the ^{vertical} 'poles' of the collar. The collars are deliberately oversized (horizontally) and undersized (vertically), so that skin tension is needed to close the yoke to yoke gap, and ~~causes~~ the yokes ~~to~~ transmit the skin tension to the collars through the horizontal interference fit. The skin stress is a critical factor, as it determines the collar-yoke and yoke-yoke loads during assembly and

operation of the magnet. Instead of constructing a structure with line to line fits when warm, the vertically split yoke magnet relies on localized interferences and clearances between the collar and yoke packs to achieve a more rigid support assembly after cooldown of the magnet. Furthermore, by creating a yoke-yoke compressive force greater than the expected Lorentz loading of the magnet, the yoke to yoke contact is always maintained, and the collar (and coil) motion due to excitation is reduced.

The goals of the mechanical analysis are then: 1) to minimize the coil motion under Lorentz loading, 2) maintain compressive loads between the collar and yoke at all times, 3) allow for a vertical collar to yoke clearance at all times, and 4) ensure the yoke to yoke split is closed after skinning of the cold mass. To achieve these goals, the finite element model has been used to determine the shape of the outside collar surface, the skin thickness and prestress necessary to close the yoke split when warm, the allowable ranges of yoke taper (which allows for proper mating of the yoke halves due to bending of the iron during assembly), and the desired shape of the coil cavity in the collar lamination for proper conductor placement after cooldown. The effect of an internal pressure on the skin, simulating quench conditions, has also been investigated.

MODEL

The 2-D ANSYS model used for these calculations is shown in figure 1. As can be seen from the different mesh patterns, the model is actually a composite. The coil and collar mesh patterns are taken directly from the horizontally split yoke design², with a few modifications in the treatment of the coil system (a

discussion of this change is documented elsewhere³, but the differences are small). The yoke and skin meshes were then generated to allow for the proper treatment of the yoke-collar interface necessary with the vertical split. Although not particularly esthetically pleasing, ~~the~~ neither of the two meshes cause any numerical distortions. A great thanks is due to Jon Turner and Giancarlo Spigo of the SSC Laboratory, for their allowance of ~~my~~ use of their work in the generation of the coil and collar sections and the calculations of the Lorentz loads used in this model.

A number of assumptions are made in the model, including constant, isotropic, and elastic material properties, frictionless contact surfaces, plane stress analysis, and Lorentz loads calculated using infinite permeability iron. Collar to yoke interference is assumed only until an azimuthal angle of 30°, after which the surfaces are free with respect to one another. Other pertinent parameters, including material properties, are listed in Table ~~A~~ 1.

RESULTS

Results are presented for four assembly and operational steps, namely Preload, which simulates the collared coil after removal from the collaring press, Skinning, which simulates the completed cold mass after removal from the yoking press, Cooldown, which simulates the conditions of the magnet at 0 T, 4°K, and Excitation, which simulates the magnet at 6.9T, 4°K. Tabulated data show the radial deflections of the collar outer edge at the horizontal and vertical planes, while plots show the loading at the collar-yoke and yoke-yoke interfaces, and the skin tensile load.

1. Effect of Skin Stress

Calculations were made for cases of varying skin stress, to determine the minimum tensile load necessary, and the allowable range of stress in the skin while ensuring magnet operation. Table 2 shows the calculated deflections for each case, while figures 2 through 4 show the collar-yoke, yoke-yoke, and skin forces associated with each case at each load step. Aside from the skin stress, all other parameters were held constant.

At the preload step, since the cases are all identical, no difference is noted in the deflections of the collared coil, and there are no loads on the yoke or skin, since they haven't been applied yet. The vertical ovalization of the collar is expected, and the magnitude of these deflections agree well with those calculated in the horizontally split design, although differences do exist due to the differences in modeling techniques. After skinning, the higher skin stresses produce greater horizontal motion of the collar, until the yoke gap closes. Before the yoke split is closed, all of the skin load is transmitted by the yoke to the collar, which deflects inward horizontally and radially outward vertically. After yoke to yoke contact, collar motion stops, and further skin loads result in higher compressive yoke-yoke loads. The increasing collar-yoke loading is apparent in figure 2, while the yoke contact appears to occur only for the highest skin stress case, resulting in a yoke-yoke load (figure 3) and decreased collar motion (table 2) and a smaller increment of collar-yoke load increase (figure 2). Further skin loading would result in higher yoke-yoke loads, but no increase in collar-yoke load or collar deflection.

Upon cooldown, the relative shrinking of the skin, yoke, collar and coil produce several effects. First, the shrinkage of the skin relative to the yoke causes the yoke interface to close for all cases of skin stress except the zero prestress case. Both the deflections, which show the collar to be in the nearly the same position for all skin loads, and the force plots, which show the identical collar-yoke load in each case support this. Differences in skin stress are reflected as differing yoke-yoke loads. The decrease in collar to yoke load from the preload case is due to the shrinkage of the collar away from the inside radius of the yoke, while the small differences in collar position are due to the differing skin stresses, which bend the yoke different amounts, and change the yoke-yoke interference at the vertical plane.

Finally, under excitation, the Lorentz loads are transmitted into increased collar-yoke loads, and offset by decreased yoke to yoke loads in all cases except where the skin initially had no prestress. The zero prestress skin case also shows an increase in collar-yoke load, however, although smaller, since the increased deflection of this system results in more of the excitation load being resisted by the stiffness of the collar packs themselves. When enough yoke to yoke compressive load existed after cooldown, the excitation of the magnet resulted in a trading of loads, minimal collar deflections, and constant skin loads. Collar deflections under excitation is 0.7 mils horizontally and -1.25 vertically, less than those predicted for the horizontally split design under the same conditions. Using the criterion of yoke interface closure when warm, these results suggest a 4.9mm skin prestressed to about 22ksi will close the yoke gap and provide the desired collar-yoke loading.

2. Effect of Skin Thickness

In another comparison, the skin thickness was increased to investigate its effect on the support of the coil. Thicknesses of 4.9mm and 6.35mm were compared, with the same displacement load placed on each. These results in skin tensile loads of 17.1ksi and 16.0ksi, respectively. All other parameters were held constant. Displacement results are shown in table 3, with forces in figures 5 through 7. The 4.9mm skin results are the same as those presented in section 1. The predictions show the increased thickness provides enough additional support to close the yoke interface (the thinner skin results in an interface that is just open), and increased loading due to cooldown, as expected. However, the loading of the thinner skin with cooldown also results in yoke interface closure, so that with excitation there is no difference in mechanical performance. Although a thicker skin provides slightly increased stiffness and decreases the skin stress necessary to close the yoke split, it does not appear to provide a great mechanical advantage over a properly stressed thinner skin, in this design.

3. Effect of Coil Preload

Since, during assembly, a range of coil preloads is acceptable, the compressive preload applied to the coil was varied to examine the effect on the system mechanics (Table 4, Figures 8 through 10). This also provides a tolerancing on the vertical gap necessary between the collar and the yoke, and the necessary horizontal interference. The higher preload case is identical to the case described in section 1 where the yoke gap is closed after skinning (highest skin stress). Table 4 shows reduced collar deflections for the lower preload case (linear with coil preload), but after skinning the collar has reached essentially the same horizontal position, although the vertical deflection is still different due to the

variation in coil stress. The forces are redistributed slightly, with more of the skin stress transferred to the collar after skinning for the lower coil stress case. Since the collar is more horizontally oval when less coil preload is applied, more of the skin forces are applied to the collar, and less into compression of the yoke to yoke split (figures 8 and 9). The yoke-yoke interface is still closed, with plenty of margin, and after cooldown and during operation, both models track each other. No difference in operation of either magnet is predicted.

4. Yoke Taper

A yoke taper of 1.25 mils along the mating surface (greater gap at the outer radius) was found to provide the best yoke to yoke mating when the bending of the yoke was accounted for after skinning. However, tapers from 0 mils (no taper) to 3 mils produced no significant effect on magnet operation, so the definition of this parameter is not critical. Due to the parting plane location on the vertical, the presence of a gap at the yoke split is not expected to have a detrimental effect on the magnetic performance of the magnet.

5. Vertical Clearance

The modeling results show a maximum collar deflection in the vertical direction of 7.58 mils after skinning, suggesting that leaving an 8 mil radial gap would (just) allow for free motion between the collar and yoke in this region. However, historically, finite element models have underpredicted the collar deflections measured on actual magnets, and since this parameter does not severely affect collar stiffness or mechanics, a 16 mil radial gap between the collar and yoke at the vertical has been designed.

6. Horizontal Interference

In a free standing state, the outside collar edge would contract almost 2.7 mils more to helium temperatures than the inside radius of the yoke. The interference fit of the collar and yoke at the horizontal must allow for this differential to maintain the desired loading scheme. The design interference of 5.5 mils radially should be more than adequate for this purpose.

7. Shaping of the Coil Cavity

Since the multipoles of the magnet are strong functions of conductor placement, the coil cavity should be shaped so the coil is in the proper position for operation. By examining the motion of the coil in the model from the initial state to the cooldown stage, an estimate of these placement corrections can be made. Another computation, using a coil preloaded to 10 ksi (the middle of the acceptable range), was completed for this purpose. Deflections change by less than ± 1 mil if the preload is at one or the other extreme from this case. For the 10 ksi case, the coil cavity deflections (cartesian coordinates, in mils) are as follows:

Inner Coil, Inner Midplane	-8.07, 10.00
Inner Coil, Inner Pole	-0.81, 1.96
Inner Coil, Outer Pole	-1.35, 0.43
Outer Coil, Inner Pole	-3.49, 1.19
Outer Coil, Outer Pole	-4.87, -0.95
Outer Coil, Outer Midplane	-10.25, 10.00

The 10 mil vertical deflections at the midplane are artifacts of the application of coil preload in the model. By correcting the collar design for the remainder of the coil deflections, good positioning of the conductor during operation can be assured.

8. Comparison with other models

A brief comparison with the results of other models is useful for corroboration of these results. As previously mentioned, good agreement with the collar deflections calculated by the horizontally split mechanical analysis has also been achieved. Another calculation, modeling the yoke and skin interaction under Lorentz loads for this geometry has also been reported⁴. A comparison of these results, the SAPIV model, and the deflections for a collar only (no yoke or skin support at any time) is shown in Table 5. The SAPIV model predicts a horizontal deflection of the yoke by 2.5 mils during excitation, while the vertical split model predicts a deflection of only 0.7 mils. However, the SAPIV model does not account for the stiffness of the collar, which also resists the Lorentz load of the coil. The collar only case presented in Table 5 shows the collar to be a relatively stiff support member, which has a non-negligible effect on the support structure. A summing of the loads transmitted between the collar and the yoke show that only 45% of the total Lorentz load is transmitted to the yoke by the collar. A linear scaling of the SAPIV results by this amount reduces the predicted deflection to 1.125 mils. Furthermore, the load is actually transmitted as a distributed load, instead of as a point load as used in the SAPIV model. Taking these two effects into account, the good agreement is found between the two models.

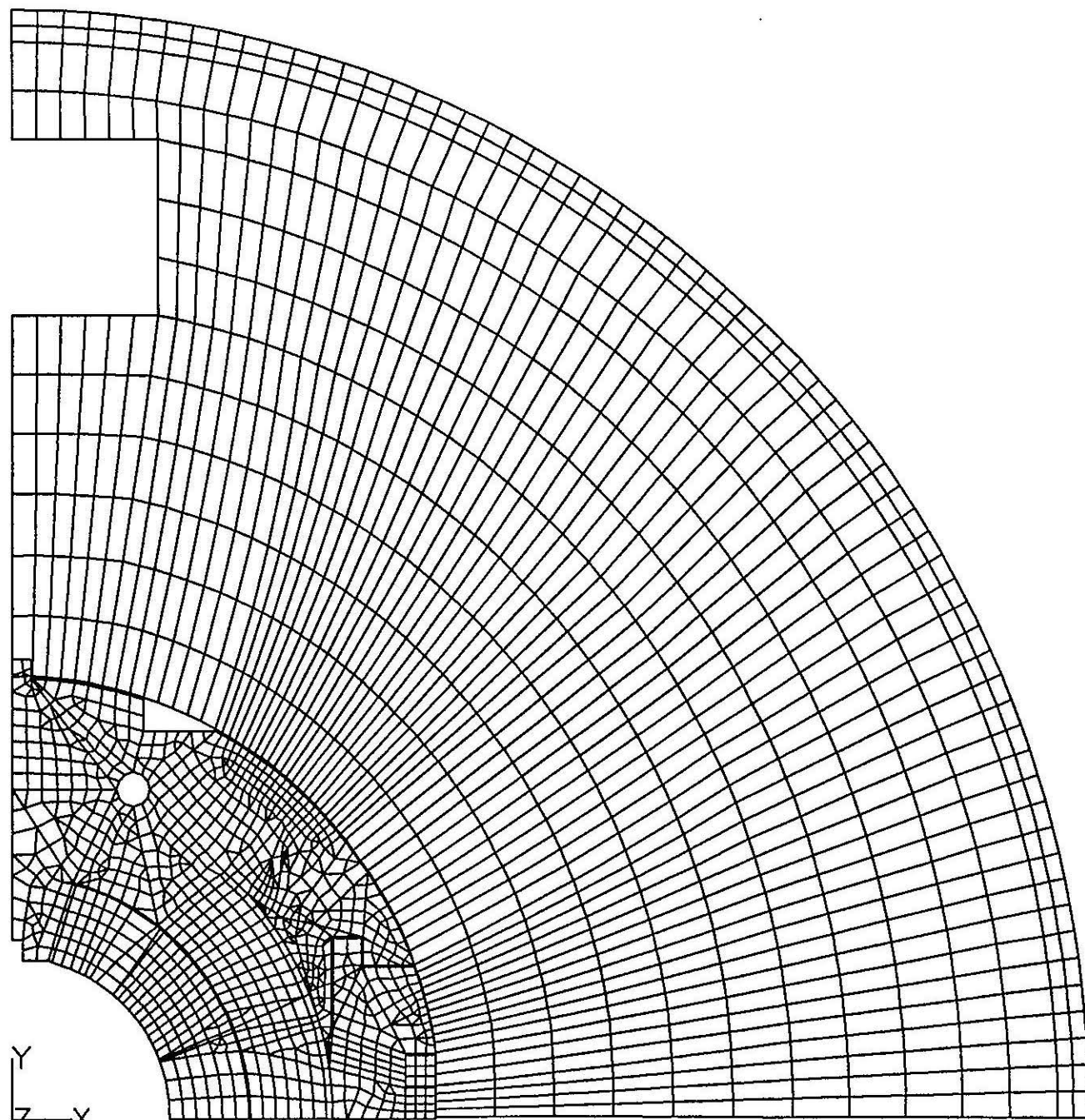
9. Effect of Quench Pressures on Support System

Concerns about the effect of a quench pressure (300 psi) on the system mechanics resulted in an additional load step being inserted in the model, which had a pressure load on the inner surface of the cold mass skin. If large enough, this pressure could reduce the skin load on the yoke, which would reduce the yoke to yoke loading and the collar to yoke loading. However, the 300 psi design pressure for the SSC magnet was not large enough to do this, as it changes the yoke to yoke loading by only 2000 lb/axial inch. Quenches should have no permanent effect on the cold mass mechanics.

CONCLUSIONS

The finite element model of the 50mm vertically split dipole gives good agreement on collar deflections with two other, independently created models. The results suggest that a 4.9 mm skin, prestressed when warm to 22 ksi, will close the yoke to yoke gap. Oversizing the collar 5.5 mils horizontally, and undersizing the collar 16 mils vertically, will supply the necessary geometry to take full advantage of the vertically split yoke support mechanism. Furthermore, the coil cavity of the collar can be shaped to provide for optimum field quality during operation of the magnet.

1



DSX elements

ANSYS 4.4
MAY 21 1990
07:20:33
PLOT NO. 1
PREP7 ELEMENTS
TYPE NUM

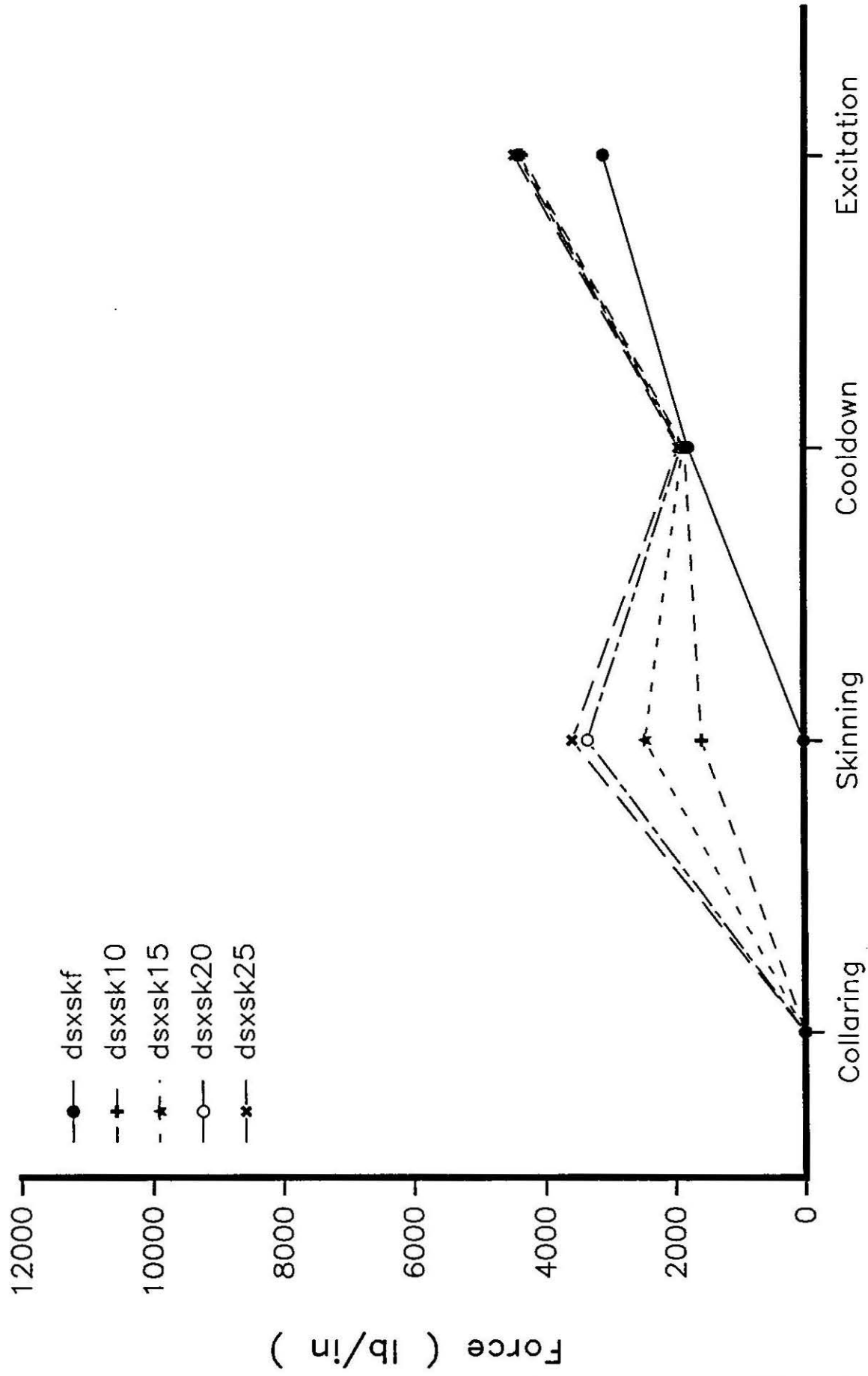
ZV =1
DIST=93.5
XF =85
YF =85

Collar Horizontal and Vertical Displacements
4.9mm Skin 13ksi Coil Preload
Varying Skin Prestress

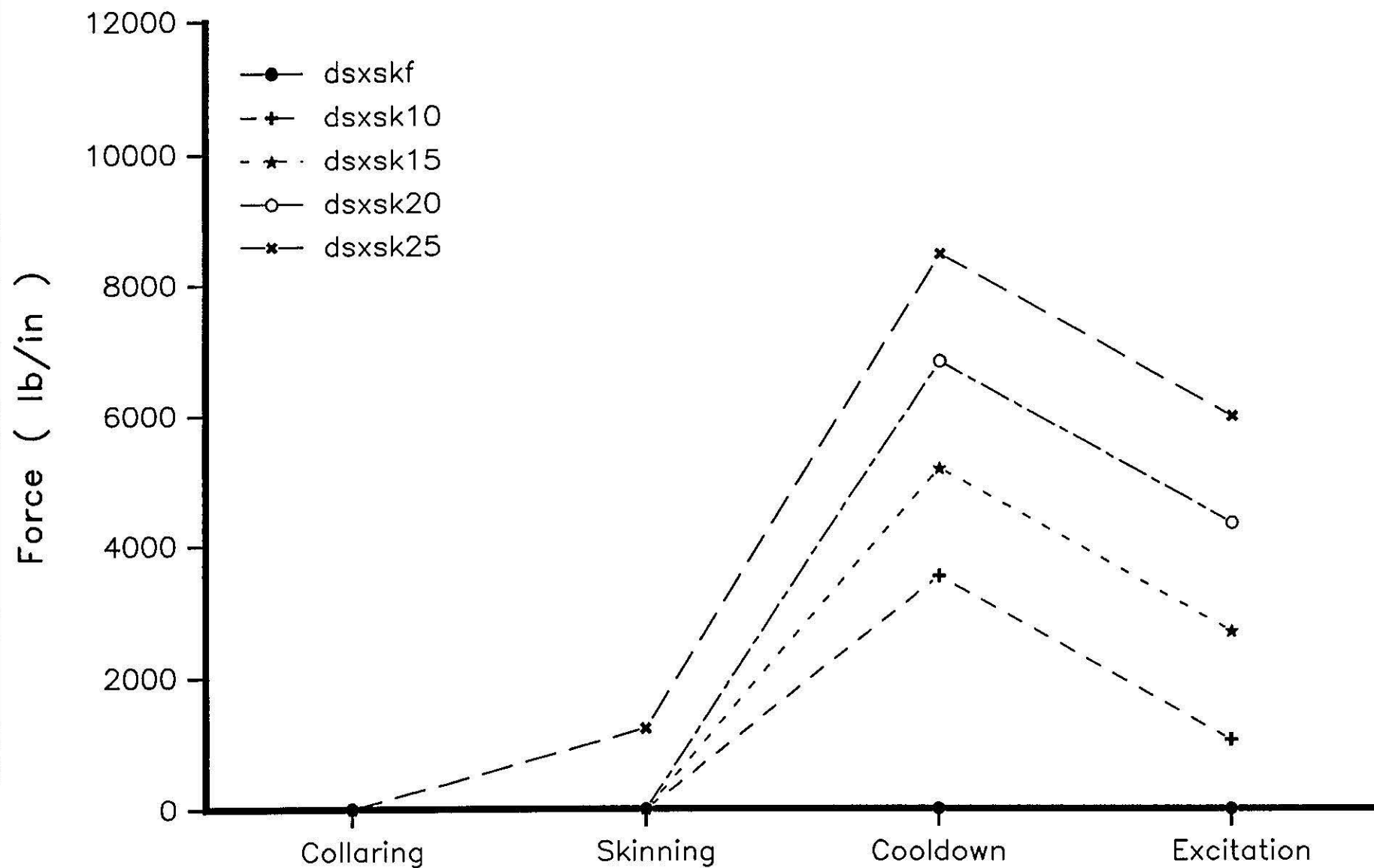
<i>Preload</i>	$\overset{H}{\text{N472}}$	$\overset{V}{\text{N689}}$		
dsxskf	-0.69 (-.017)	4.60 (.117)		
dsxsk10	-0.69 (-.017)	4.60 (.117)		
dsxsk15	-0.69 (-.017)	4.60 (.117)		
dsxsk20	-0.69 (-.017)	4.60 (.117)		
dsxsk25	-0.68 (-.017)	4.60 (.117)		
<i>Skinning</i>	N472	N689	ΔH	ΔV
dsxskf	-0.69 (-.017)	4.60 (.117)	0.00	0.00
dsxsk10	-3.10 (-.079)	5.93 (.151)	-2.41	1.33
dsxsk15	-4.39 (-.111)	6.65 (.169)	-3.70	2.05
dsxsk20	-5.63 (-.143)	7.37 (.187)	-4.94	2.77
dsxsk25	-5.98 (-.152)	7.58 (.193)	-5.30	2.98
<i>Cooldown</i>	N472	N689	ΔH	ΔV
dsxskf	-11.68 (-.297)	-2.98 (-.076)	-11.0	-7.58
dsxsk10	-11.77 (-.299)	-2.93 (-.074)	-8.67	-8.86
dsxsk15	-11.81 (-.300)	-2.90 (-.074)	-7.42	-9.55
dsxsk20	-11.86 (-.301)	-2.88 (-.073)	-6.23	-10.25
dsxsk25	-11.91 (-.302)	-2.87 (-.073)	-5.93	-10.45
<i>Excitation</i>	N472	N689	ΔH	ΔV
dsxskf	-9.21 (-.234)	-5.18 (-.131)	2.47	-2.20
dsxsk10	-11.06 (-.281)	-4.15 (-.105)	0.71	-1.22
dsxsk15	-11.11 (-.282)	-4.11 (-.105)	0.70	-1.21
dsxsk20	-11.16 (-.284)	-4.09 (-.104)	0.70	-1.21
dsxsk25	-11.21 (-.285)	-4.06 (-.103)	0.70	-1.19

$-.221 \text{ mils/ksi} = 0.82 \times 10^{-3} \text{ mm/MPa}$

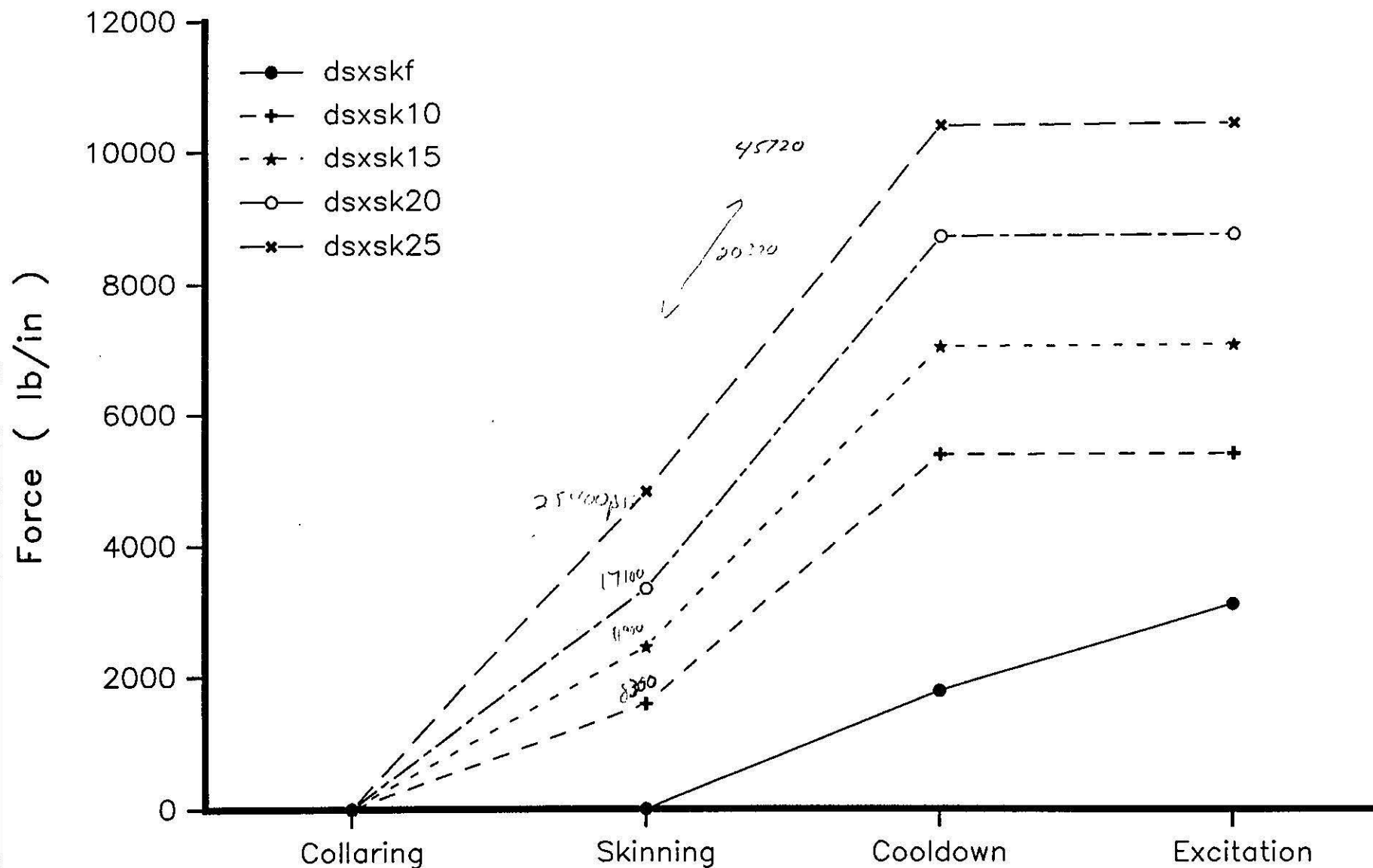
Collar / Yoke Forces



Yoke Gap Forces



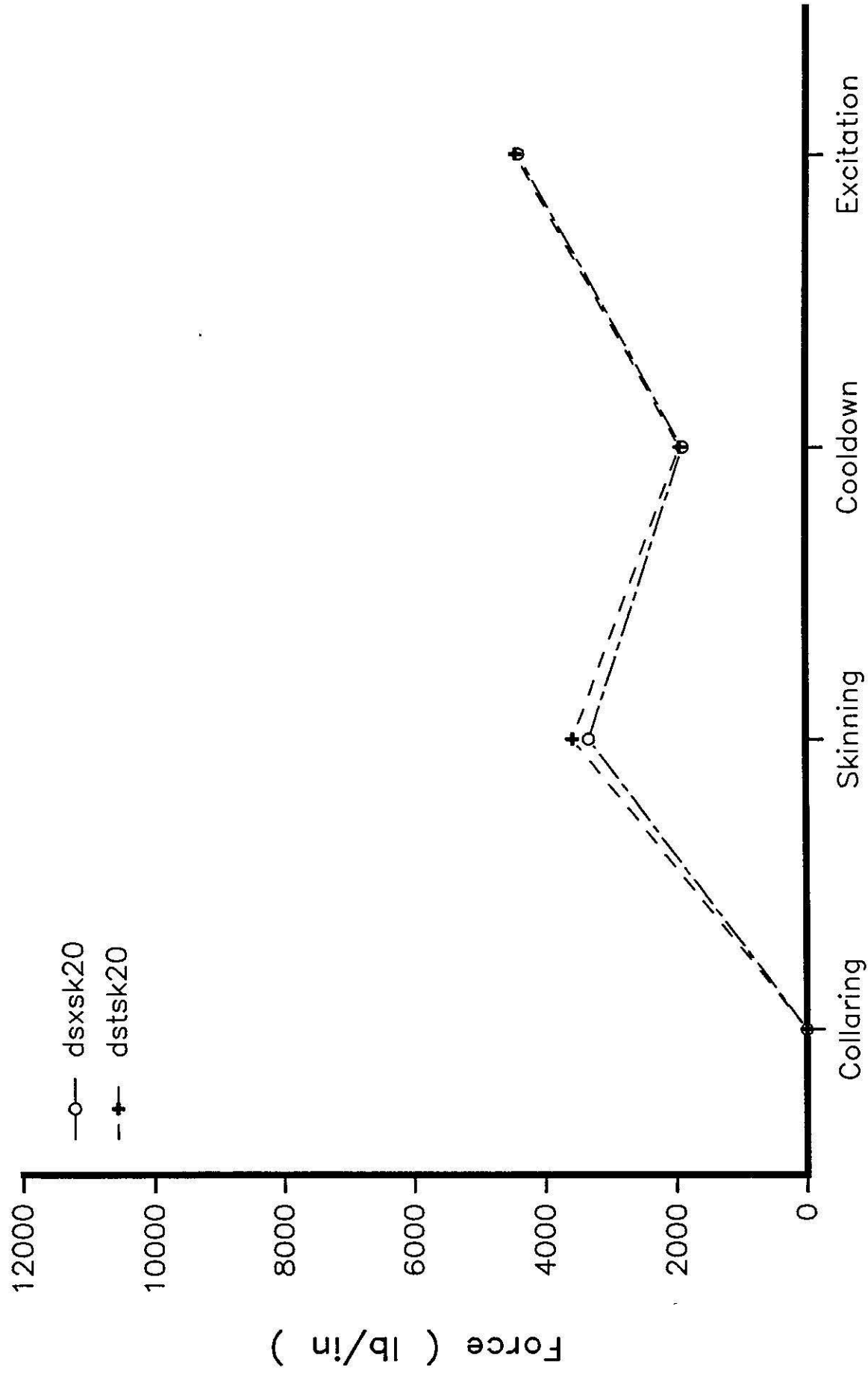
Skin Forces



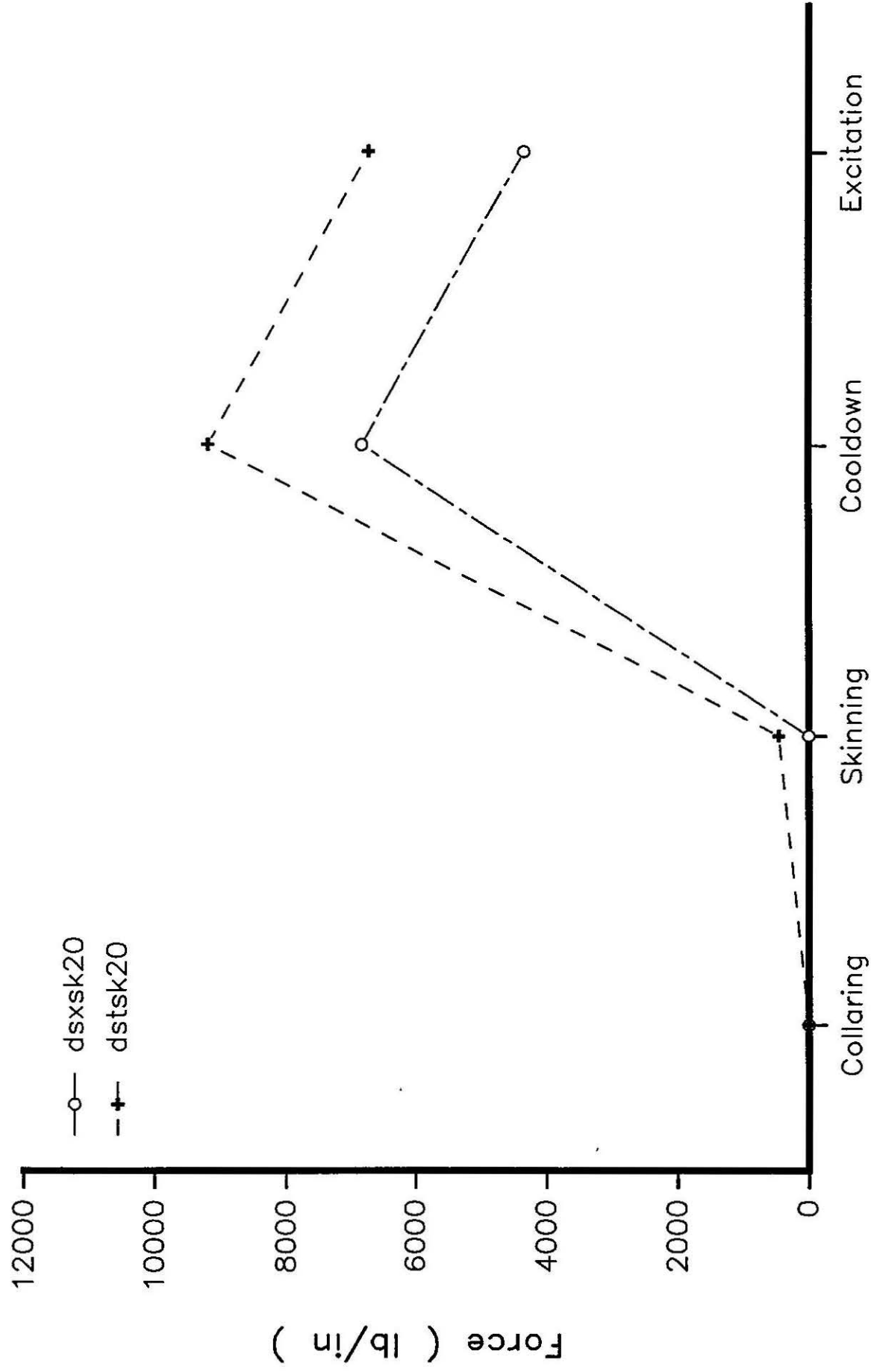
Collar Horizontal and Vertical Displacements Varying Skin Thickness

<i>Preload</i>	N472	N689		
4.90 mm skin	-0.69 (-.017)	4.60 (.117)		
6.35 mm skin	-0.69 (-.017)	4.60 (.117)		
<i>Skinning</i>	N472	N689	ΔH	ΔV
4.90 mm skin	-5.63 (-.143)	7.37 (.187)	-4.94	2.77
6.35 mm skin	-5.95 (-.151)	7.56 (.192)	-5.27	2.96
<i>Cooldown</i>	N472	N689	ΔH	ΔV
4.90 mm skin	-11.86 (-.301)	-2.88 (-.073)	-6.23	-10.25
6.35 mm skin	-11.93 (-.303)	-2.84 (-.072)	-5.98	-10.40
<i>Excitation</i>	N472	N689	ΔH	ΔV
4.90 mm skin	-11.16 (-.284)	-4.09 (-.104)	0.70	-1.21
6.35 mm skin	-11.23 (-.285)	-4.05 (-.103)	0.70	-1.21

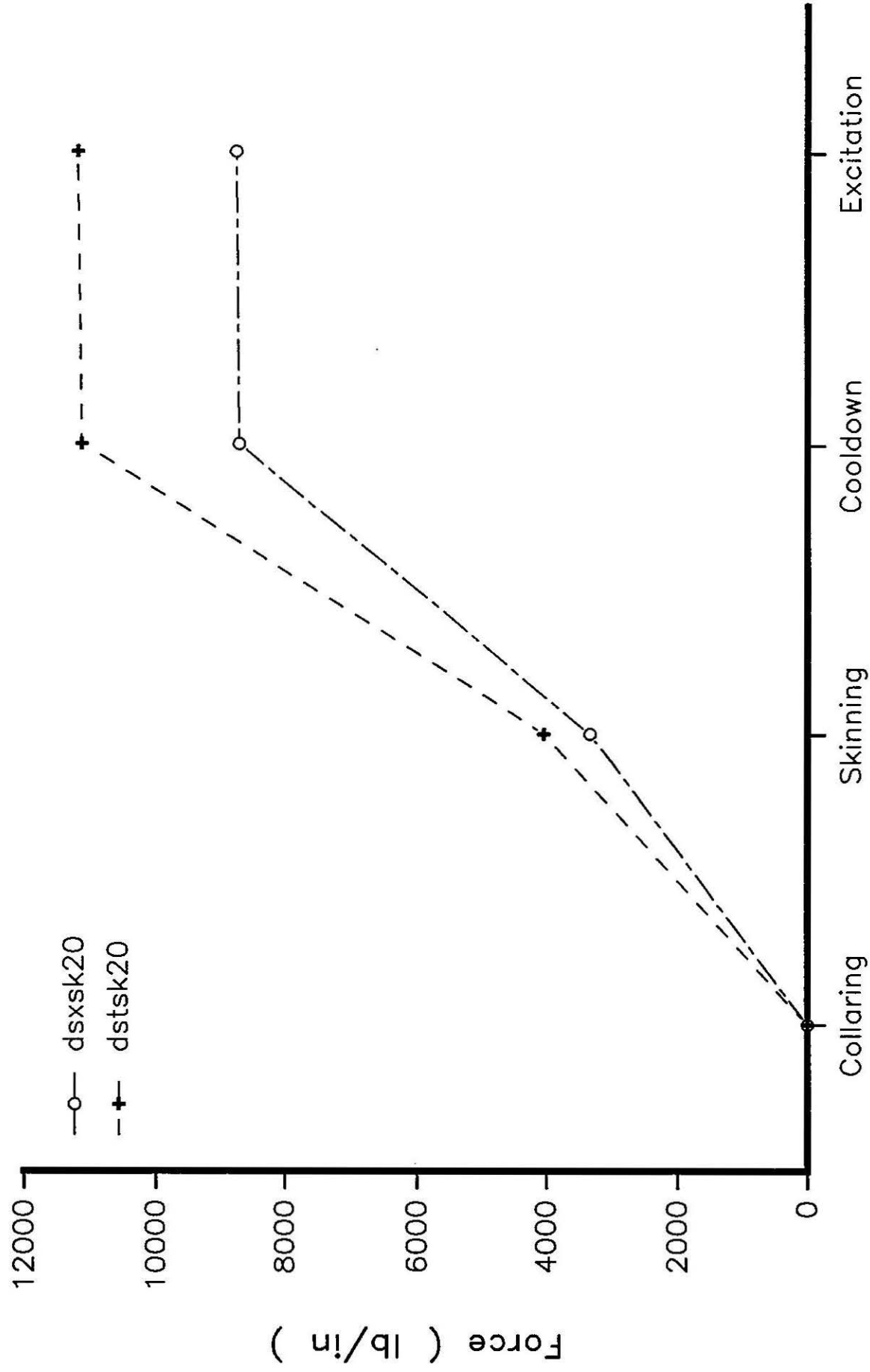
Collar / Yoke Forces



Yoke Gap Forces



Skin Forces



Collar Horizontal and Vertical Displacements

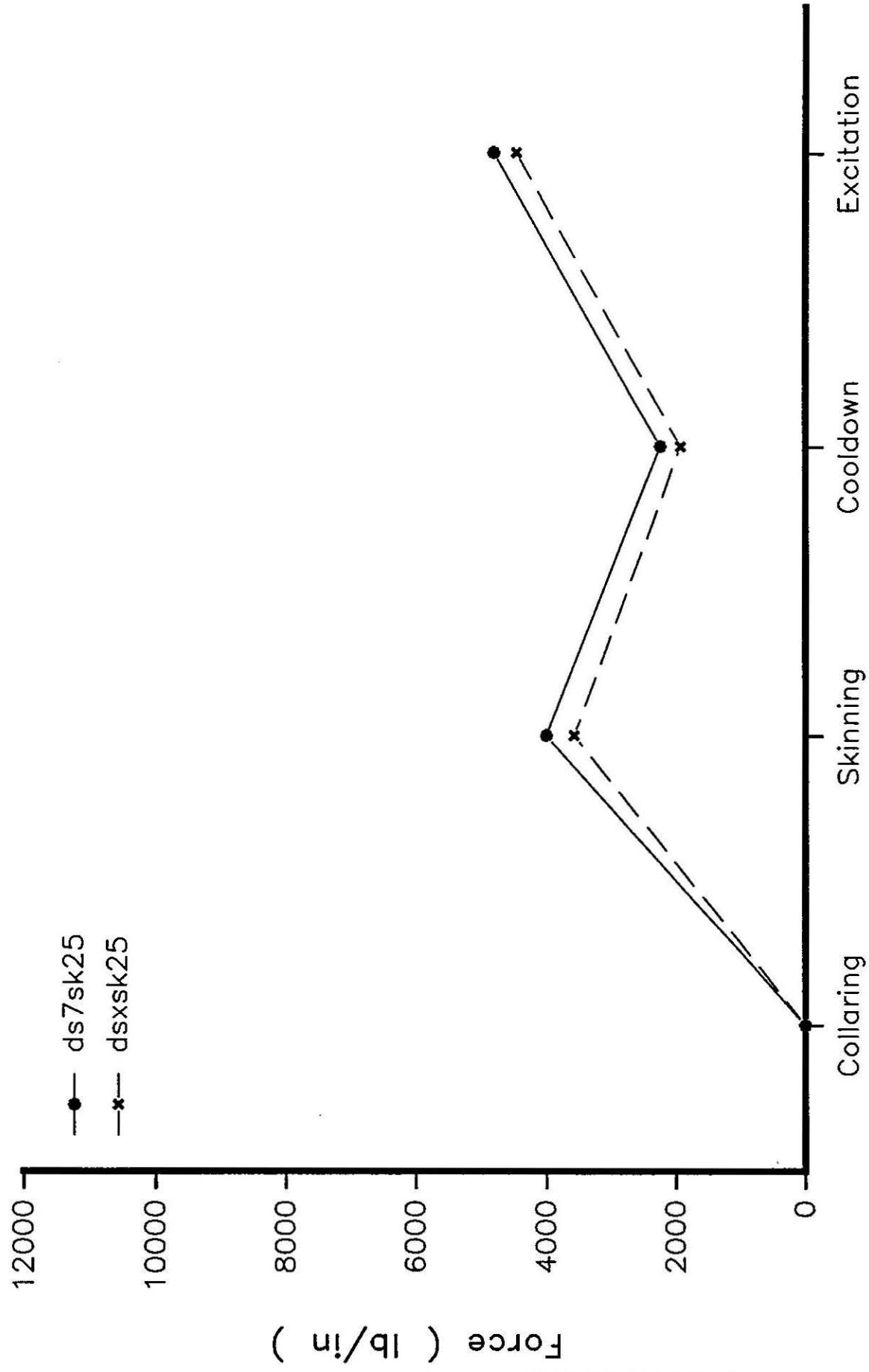
Varying Coil Preload 4.9mm Skin 25 ksi Prestress

<i>Preload</i>	N472	N689		
7. ksi coil	-0.37 (-.009)	2.48 (.063)		
13. ksi coil	-0.68 (-.017)	4.60 (.117)		
<i>Skinning</i>	N472	N689	ΔH	ΔV
7. ksi coil	-5.83 (-.148)	5.71 (.145)	-5.46	3.23
13. ksi coil	-5.98 (-.152)	7.58 (.193)	-5.30	2.98
<i>Cooldown</i>	N472	N689	ΔH	ΔV
7. ksi coil	-11.76 (-.299)	-4.77 (-.121)	-5.93	-10.48
13. ksi coil	-11.91 (-.302)	-2.87 (-.073)	-5.93	-10.45
<i>Excitation</i>	N472	N689	ΔH	ΔV
7. ksi coil	-11.11 (-.282)	-5.94 (-.151)	0.65	-1.17
13. ksi coil	-11.21 (-.285)	-4.06 (-.103)	0.70	-1.19

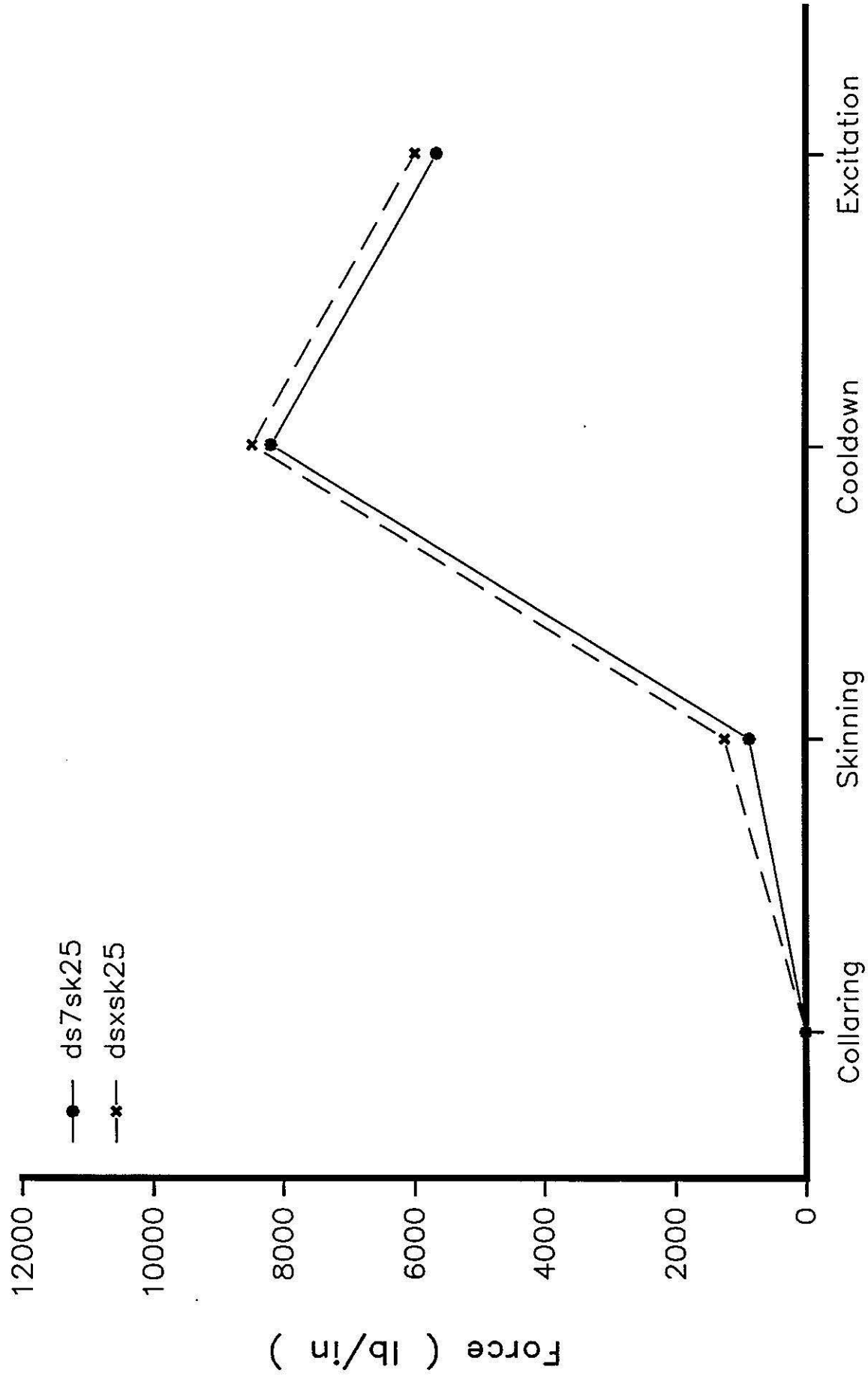
$$\begin{array}{r} .0117 \\ .0063 \\ \hline .054 \end{array} = \Delta r_v \rightarrow \Delta d_v = .108 \text{ mm}$$

$$\begin{array}{r} .017 \\ .009 \\ \hline .008 \end{array} = \Delta r_h \rightarrow \Delta d_h = .016$$

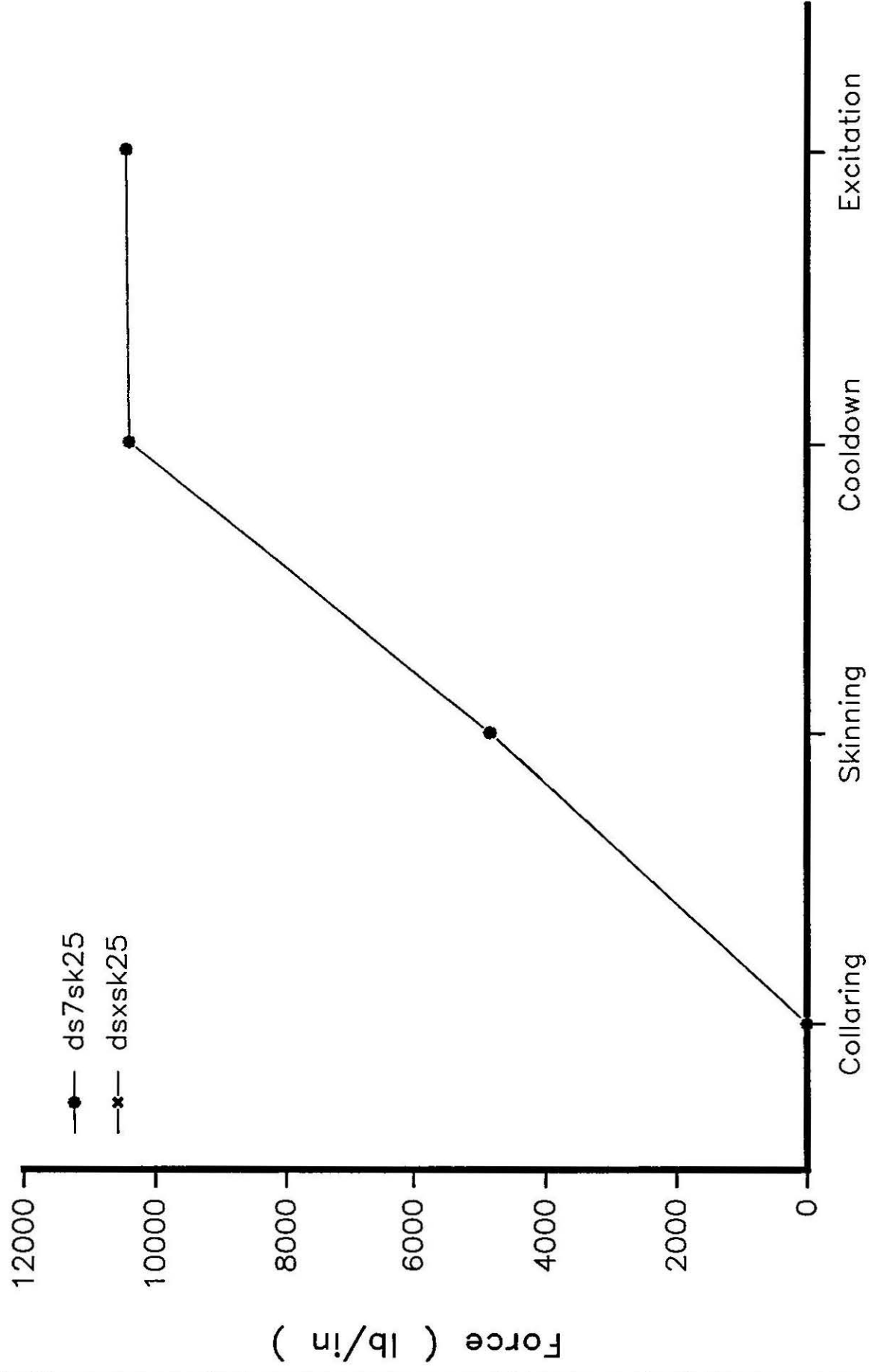
Collar / Yoke Forces



Yoke Gap Forces



Skin Forces



Collar Horizontal and Vertical Displacements

<u>Preload</u>	<u>N472</u>	<u>N689</u>		
collar	-0.67 (-.017)	4.59 (.117)		
dsxsk25	-0.68 (-.017)	4.60 (.117)		
<u>Skinning</u>	<u>N472</u>	<u>N689</u>	<u>ΔH</u>	<u>ΔV</u>
collar	-0.67 (-.017)	4.59 (.117)	0.00	0.00
dsxsk25	-5.98 (-.152)	7.58 (.193)	-5.30	2.98
<u>Cooldown</u>	<u>N472</u>	<u>N689</u>	<u>ΔH</u>	<u>ΔV</u>
collar	-8.99 (-.228)	-4.47 (-.114)	-8.32	-9.06
dsxsk25	-11.91 (-.302)	-2.87 (-.073)	-5.93	-10.45
SAPIV			-5.8	
<u>Excitation</u>	<u>N472</u>	<u>N689</u>	<u>ΔH</u>	<u>ΔV</u>
collar	-4.35 (-.111)	-7.81 (-.198)	4.64	-3.34
dsxsk25	-11.21 (-.285)	-4.06 (-.103)	0.70	-1.19
SAPIV			2.5	-1.7

$$\begin{array}{r} .228 \\ + .111 \\ \hline .339 \end{array} = \Delta H_{\text{free collar}}$$

$$\begin{array}{r} .198 \\ + .114 \\ \hline .312 \end{array} = \Delta H_{\text{free collar}}$$

$$\begin{array}{r} .302 \\ - .285 \\ \hline .017 \end{array} = \Delta H_{\text{yoke supported}}$$

$$\begin{array}{r} .103 \\ - .073 \\ \hline .030 \end{array} = \Delta H_{\text{yoke supported}}$$